PCCP

Cite this: *Phys. Chem. Chem. Phys.*, 2012, **14**, 10187–10195

www.rsc.org/pccp

PAPER

Hydrogen bond dynamics in crystalline β-9-anthracene carboxylic acid—a combined crystallographic and spectroscopic study†

René Moré,‡*[a] Mirko Scholz,‡[a] Gehard Busse,[a] Lennart Busse,[a] Carsten Paulmann,[bc] Martin Tolkiehn[d] and Simone Techert[a]

Received 21st January 2012, Accepted 18th May 2012
DOI: 10.1039/c2cp40216e

We compare results from single crystal X-ray diffraction and FTIR spectroscopy to elucidate the nature of hydrogen bonding in β-9-anthracene carboxylic acid (β-9AC, $C_{15}H_{10}O_2$). The crystallographic studies indicate a disorder for the protons in the cyclic hydrogen bond. This disorder allows the determination of the energy difference between two proton sites along the hydrogen bond. The temperature dependent Fourier transform infrared spectroscopy (FTIR) underpins the crystallographic results. The combination of both methods allows the estimation of a one-dimensional potential curve describing the OH-stretching motion. The dynamical properties of the proton transfer along the hydrogen bond are extracted from this potential. The work presented here has profound implication on future studies of photochemical dynamics of crystalline β-9AC, which can deliver a deeper understanding of the mechanism of photochemical driven molecular machines and the optical and electronic properties of molecular organic semiconductors.

Introduction

Since the pioneering work of Latimer and Rodebush[1] in 1920 the concept of hydrogen bonding has played an important role in many biological and chemical systems.[2–8] Hydrogen bonds have a significant influence on the thermodynamic, electrical and optical properties of matter. They are some of the major building blocks in living nature. In amino acids the proton transfer is essential for the isomerization from neutral amino acid to their zwitterionic form. Calculations based on the reaction force framework show that bridging water molecules stabilize the zwitterionic form of amino acid and increases the reaction barriers.[8] In DNA formation of hydrogen bonds is a major structural property and the double proton transfer plays a crucial role as a potential precursor for spontaneous mutation.[7]

Cyclic carboxylic acid dimers are some of the most investigated hydrogen bond architectures, which are ideal systems to study a double proton transfer in detail. In the case of an isolated centrosymmetric system, it can be described by a symmetric double-well potential (see Fig. 1). In a crystal lattice, the crystal field caused by the neighboring molecules breaks the symmetry. This leads to the fact that in a crystal lattice such a centrosymmetric system is described by an asymmetric double-well potential.[6,9–12] The major parameters describing this asymmetric potential are the activation energy E_A and the energy difference ΔG (see Fig. 1). Potassium bicarbonate ($KHCO_3$) and benzoic acid (C_6H_5COOH) are well-established model systems for such hydrogen bonded dimers in the solid state. These systems are studied with various experimental techniques like solid-state NMR,[11,12] vibrational spectroscopy,[9,10] X-ray diffraction,[13] optical spectroscopy[11,14] and quasi elastic neutron scattering (QENS).[6,15] Especially with vibrational spectroscopy it is possible to investigate the quantum dynamics of the proton transfer along such a hydrogen bond. In the reaction path model the proton transfer is represented as a chemical equilibrium between uncorrelated tautomers.[16] The proton is treated as a dimensionless particle in this semiclassical picture. The reorganization of single-bond and double-bond structure during the proton transfer defines a multi-dimensional reaction coordinate. This multi-dimensional reaction coordinate is represented by ζ in Fig. 1. For the description of QENS and solid state NMR experiments a phonon assisted model was introduced.[11] In this model, the proton transfer is monitored by displacements of the heavy atoms coupled to the thermal bath. At low temperature

[a] *Max-Planck-Institut für biophysikalische Chemie, Strukturdynamik (bio)chemischer Systeme, Am Fassberg 11, 37070 Göttingen, Germany. E-mail: rmore@gwdg.de*
[b] *Hasylab, Notkestr. 85, 22607 Hamburg, Germany*
[c] *Mineralogisch-Petrographisches Institut, Universität Hamburg, Grindelallee 48, 20146 Hamburg, Germany*
[d] *Deutsches Elektronensynchrotron DESY, FS-DO, Notkestr. 85, 22607 Hamburg, Germany*

† Electronic supplementary information (ESI) available. CCDC 863712 (50 K, D3), 863719 (75 K, D3), 863725 (100 K, F1), 863813 (135 K, D3), 863814 (150 K, D3), 863815 (155 K, D3), 863816 (205 K, D3), 863817 (230 K, D3), 863818 (250 K, D3), 863819 (255 K, D3), 863820 (255 K, D3), 863821 (140 K, F1), 863822 (180 K, F1) 863823 (230 K, F1) and 863824 (260 K, F1). For ESI and crystallographic data in CIF or other electronic format see DOI: 10.1039/c2cp40216e

‡ These authors contributed equally to this work.

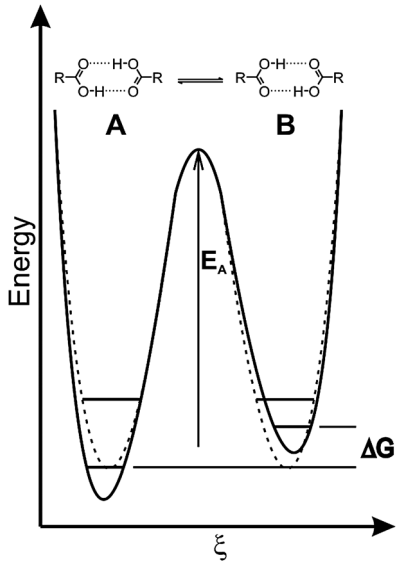

Fig. 1 Schematic potential for the cyclic hydrogen bonded carboxylic acid dimer. The dashed line represents the symmetric potential for an isolated carboxylic acid dimer and the solid line shows the potential for the carboxylic acid dimer in the solid state, having an asymmetry caused by the crystal field. The scheme has been adapted from Fillaux *et al.*[9]

the rate for proton transfer is coupled by incoherent tunneling and at higher temperature by a classical Arrhenius over the barrier process, which is mentioned in Fig. 1. Nonetheless neutron diffraction experiments did not observe for $KHCO_3$ and benzoic acid a destruction of a long range space coherence of protons and dimers caused by a stochastic disorder.[16–19] Based on spectroscopic results a quantum mechanism for the proton transfer based on coherent tunneling of pseudoprotons was developed.[9,10,20] This mechanism is based on a quasi-symmetric potential describing the OH-stretching motion, which should not be confused with the schematic potential in Fig. 1. This coherent tunneling model shows similar description for the rate of proton transfer reaction based on the parameter of quasi-symmetric potential.[9]

The aim of the present investigation is a further step towards understanding the nature of the ground state potential of crystalline β-9-anthracenecarboxylic acid (β-9AC, $C_{15}H_{10}O_2$) (Fig. 2). 9AC has interesting photochemical properties which can be influenced by the hydrogen bonding. So β-9AC undergoes a photodimerization which leads selectively to the thermally unstable head–head product.[21] This behavior suggests a topochemical reaction. Crystals of β-9AC have been shown to perform thermally reversible photomechanical motions.[22–24] Nonetheless we could show that no single-crystal to single-crystal transformation occurs and photochemical kinetics is characterized by an autoinhibition caused by increase of disorder. We predicted by DFT calculations three different conformers of the photo-product from the photodimerization of β-9AC.[25] These conformers differ only in the dihedral angle of the carboxylic acid groups and their formation can be explained by a proton transfer coupled with photodimerization of β-9AC. With a deeper understanding of the mechanism of the proton transfer and the structure of potential surface, it will be possible to draw a better picture of the complex

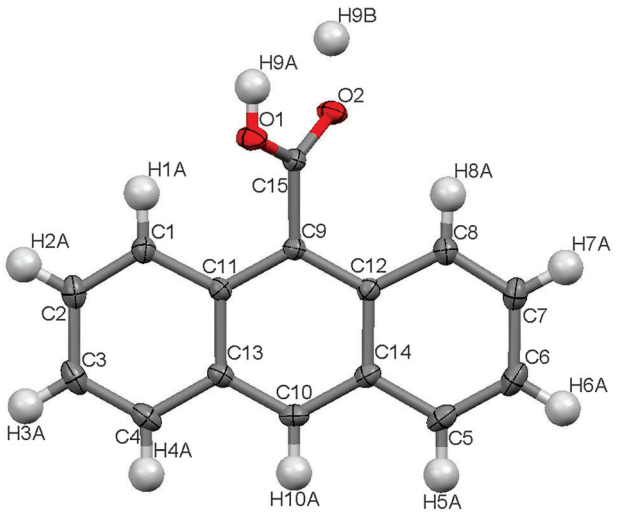

Fig. 2 ORTEP-plot of the 9AC molecule showing the atomic numbering and 50% probability ellipsoids at 180 K.

photochemistry of this system. For the investigation of hydrogen bonding properties of β-9AC we use temperature dependent crystallographic methods, which will be compared with the results from vibrational spectroscopy. Our experimental results are interpreted by use of the well devolved models for benzoic acid and $KHCO_3$.

Experimental section and data evaluation

9AC (Sigma-Aldrich) was purified by sublimation in a vacuum. The FTIR spectra were recorded with a Bruker IFD 25 FTIR spectrometer. The samples for the FTIR measurements consist of powdered β-9AC dispersed in KBr-pellets. They were placed in a cryostat (Oxford Instruments, Mikrostat HE) and cooled with liquid Helium down to 15 K.

The crystallographic experiments were carried out at the beamlines D3 and F1 at the DORIS storage ring at HASYLAB/DESY. Details about the experimental setup can be found elsewhere.[25,26] β-9AC single crystals suitable for X-ray diffraction were obtained by recrystallization from toluene. The X-ray diffraction data were collected at different temperatures from 270 K down to 50 K using a two-dimensional detector (MarCCD 165) at a wavelength of 0.6 Å. The single diffraction data were indexed and integrated with the program package XDS.[27] The crystal structures were solved and refined with the SHELXTL program package.[28]

Computational details

The density functional theory (DFT) calculations of the hydrogen bonded dimer of β-9AC have been performed by applying the computer program Gaussian09.[29] For our study the B3PW93 DFT approach was employed with the 6-311G(d,p) basis set for geometry optimization and frequency calculation. The B3PW93 functional was chosen because this functional recovers most of the dispersion energy.[30,31] This makes this functional a good choice for deriving intermolecular interaction energies. The DFT calculations have been performed in order to rationalize the experimental findings in the IR spectra. The energy levels

and the wave functions for OH stretching motion were calculated by applying the variational method[9] using a linear combination of 40 harmonic wave functions with the fundamental frequency ω_0. For these parameters the harmonic frequency of OH stretching motion, based on the DFT calculations, was used.

Results and discussion

Temperature dependent structural investigation by X-ray diffraction

According to the crystallographic results there is no structural phase transition present in the temperature regime from room temperature down to 50 K. β-9AC can actually exist in two different polymorphs,[24] a triclinic and a monoclinic polymorph. We obtained only crystals with the monoclinic space group $P2_1/n$ with four molecules in the unit cell. The crystal data and refinement parameters for the different temperature are presented in Table 1. A look at thermal evolution of the unit cell parameters shows a significant change in the β angle. This angle drops at lower temperature, almost reaches 90° at 155 K and increases again. The reason for the increase towards 50 K, however, is the definition for a proper monoclinic cell ($\beta > 90°$) which inverts the direction of the a-axis. In the case of a constant unit cell orientation over the whole temperature range and allowing for a non-standard monoclinic cell the β angle would drop from 90.47(3)° at 270 K to 89.532(3)° ($180° - \beta$) at 75 K. The twin law was applied for the structure at 155 K and no sign for twinning was found. Hence no other evidence for a structural phase transition in the observed temperature range could be observed. In Fig. 3, a view down the crystallographic a-axis of the crystal structure of β-9AC is shown. Two 9AC molecules form a centrosymmetric cyclic hydrogen bonded dimer. The red ellipse highlights the carboxylic acid dimer.

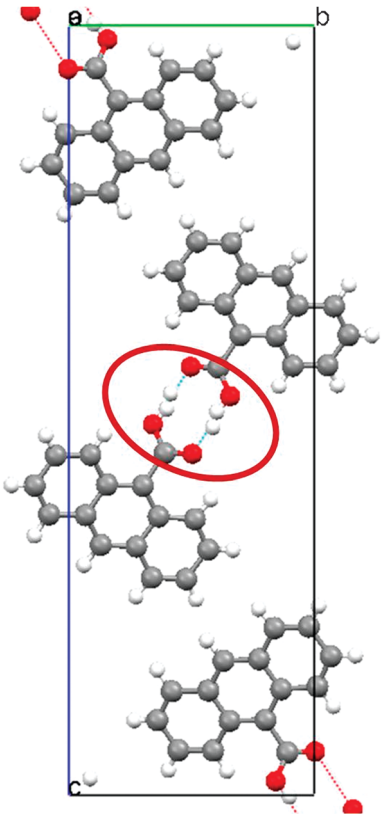

Fig. 3 Crystal structure of β-9AC viewed down the a-axis showing centrosymmetric hydrogen-bonded dimers along the c-axis. The red ellipse highlights the cyclic hydrogen bond dimer.

The intermolecular distance between the oxygen atoms in this dimer is 2.636(1) Å at 50 K, which is reasonable for a carboxylic acid dimer. The distance between the oxygen atoms is 0.019 Å

Table 1 Crystal data and refinement parameters of 9AC for different temperatures

T/K	50	75	100	135	140	150	155	180
a/Å	3.8100(8)	3.812(8)	3.835(8)	3.834(8)	3.842(8)	3.841(8)	3.840(8)	3.855(8)
b/Å	9.2900(19)	9.289(19)	9.333(19)	9.298(19)	9.335(19)	9.303(19)	9.310(19)	9.338(19)
c/Å	28.770(6)	28.754(6)	28.895(6)	28.774(6)	28.907(6)	28.797(6)	28.840(6)	28.925(6)
β/degrees	90.51(3)	90.468(3)	90.230(3)	90.153(3)	90.140(3)	90.250(3)	90.030(3)	90.100(3)
V/Å^3	1018.3(4)	1018.14	1034.2	1025.75	1036.7	1029.0	1031.0	1041.2
Z	4	4	4	4	4	4	4	4
Space group	$P2_1/n$	$P2_1/n$	$P2_1/n$	$P2_1/n$	$P2_1/n$	$P2_1/n$	$P2_1/n$	$P2_1/n$
Measured reflections	2979	2178	6795	2301	6668	2325	2746	6698
Unique reflections	2498	1823	5031	1842	4838	1954	2181	4507
R1/%	6.36	4.24	5.15	5.83	5.26	5.37	4.24	5.15
wR1/%	20.52	11.57	15.53	11.22	14.97	11.28	10.88	14.78
GooF	1.105	1.097	1.024	1.023	1.075	1.059	1.051	1.073

T/K	205	230	230	250	255	260	270
a/Å	3.8600(8)	3.8540(8)	3.8730(8)	3.8590(8)	3.8700(8)	3.8790(8)	3.8670(8)
b/Å	9.3200(19)	9.3170(19)	9.3470(19)	9.3210(19)	9.3300(19)	9.3410(19)	9.3240(19)
c/Å	28.890(6)	28.851(6)	28.975(6)	28.860(6)	28.930(6)	28.998(6)	28.882(6)
β/degrees	90.27(3)	90.26(3)	90.37(3)	90.35(3)	90.55(3)	90.53(3)	90.47(3)
V/Å^3	1039.3(4)	1036.0(4)	1048.9(4)	1038.1(4)	1044.5(4)	1050.7(4)	1041.3(4)
Z	4	4	4	4	4	4	4
Space group	$P2_1/n$	$P2_1/n$	$P2_1/n$	$P2_1/n$	$P2_1/n$	$P2_1/n$	$P2_1/n$
Measured reflections	3660	2350	6761	2348	3684	6779	2366
Unique reflections	2679	1740	4315	1632	2470	3803	1667
R1/%	4.82	4.3	5.13	4.61	4.83	5.63	5.07
wR1/%	12.69	9.66	15.06	9.87	12.3	16.88	10.91
GooF	1.052	1.053	1.048	1.014	1.020	1.027	1.038

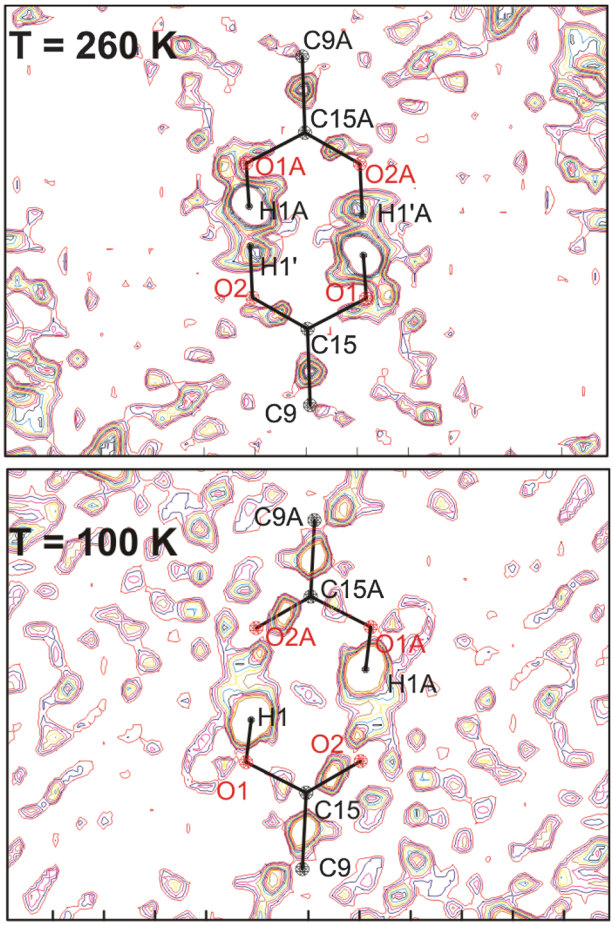

Fig. 4 Difference electron density map showing the possible hydrogen site in the hydrogen bonding network (each level 0.05 e $Å^{-3}$, from 0.25 e $Å^{-3}$ to 0.9 e $Å^{-3}$).

longer than in benzoic acid.[18,19] This difference shows that the hydrogen bond in β-9AC is slightly weaker than in benzoic acid. The β-9AC dimers have C_i symmetry caused by the dihedral angle of the carboxylic acid group. In Fig. 4, an electron density difference map around the carboxylic acid group is shown for different temperatures. At 260 K two possible proton sites are clearly visible in the difference map. These two proton sites allow a disorder caused by a strong hydrogen bonding between the two carboxylic groups of β-9AC. We introduced two occupancy sites for the two tautomeric sites. The site occupation factors were refined as a free variable.[28] In an earlier work the equilibrium constant $K_a = 0.569$ for the proton transfer along a hydrogen bond was extracted from the occupation factor.[25] With the equilibrium constant we calculated the Gibbs energy of the double-well potential yields *via* $\Delta G = -RT\ln(K_a)$ to be $\Delta G = (106 \pm 10)$ cm^{-1}. In the difference electron density map at 100 K a second proton site is not clearly observable. An increase in the electron density is visible on the C15–O2 bond, which can be explained by a stronger double bond character at low temperatures for this bond. The temperature dependence of the bond lengths in the carboxylic acid group shows the same picture. Nonetheless, it is necessary to take into account that hydrogen atoms are problematic to locate in X-ray diffraction because of their low X-ray scattering factor. With low temperature and high-resolution data it is possible to determine isotropic displacement parameters for hydrogen atoms. Anisotropic displacement parameters (ADPs) for hydrogen atoms can be estimated utilizing the SHADE web server.[32,33] We used the SHADE web server to estimate ADPs for the hydrogen atoms in the low temperature structures. Fig. 5 shows a packing diagram of 9AC at 50 K. In this packing short C–H···O intermolecular hydrogen bonds of ~2.6 Å are visible. Similar C–H···O intermolecular contacts are also reported for benzoic acid.[18]

In the temperature dependent crystal structure a significant change in the bond length in the carboxylic acid group is visible. The nominally single (C–O) bond lengthens with decreasing temperature, while the double bond (C═O) is reduced with decreasing temperature (see Fig. 6). The temperature dependence of the bond lengths can be described as follows:

$$r(\text{C–O}) \approx (0.5 + \rho(T))r_{\text{CO}} + (0.5 - \rho(T))r_{\text{single}}$$

$$r(\text{C═O}) \approx (0.5 + \rho(T))r_{\text{CO}} + (0.5 - \rho(T))r_{\text{double}} \quad (1)$$

Here ρ is the fractional occupation number of the thermodynamically unfavorable tautomer, r_{CO} is the bond length for a completely delocalized proton and r_{single} and r_{double} are the bond length of the single and the double bond, respectively, for the case of a completely localized proton. Fillaux introduced a

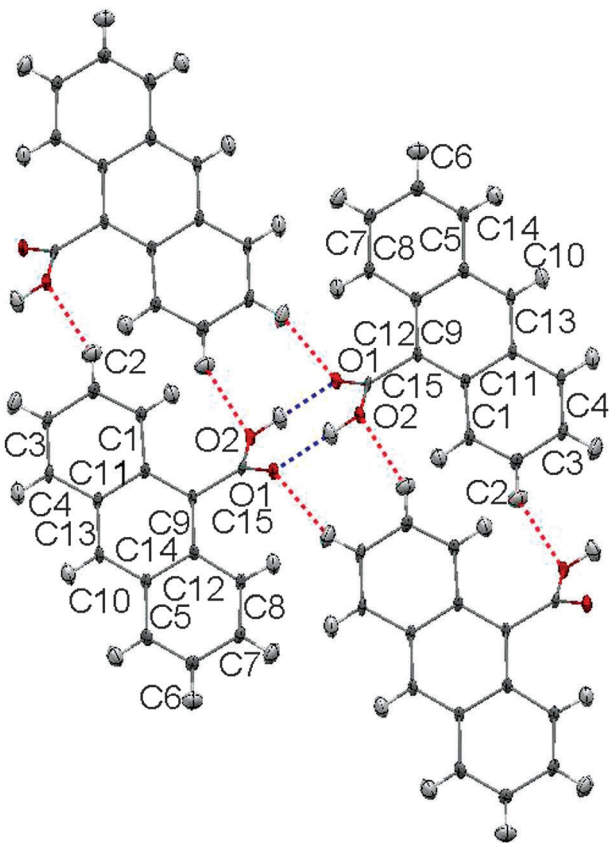

Fig. 5 Packing diagram of β-9AC structure at 50 K showing the intermolecular contacts to the oxygen atoms (red lines) and hydrogen bonds (blue lines). The ADPs of the hydrogen atoms were estimated utilizing the SHADE web server.[32,33]

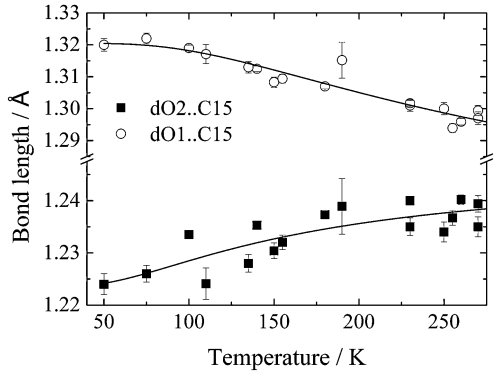

Fig. 6 Temperature dependence of the bond lengths in the carboxylic acid group. The circles represent the bond length of the single like C–O bond and the black squares represent the double like C═O bond. The black line models are based on the fit-functions (3a) and (3b) resulting in an energy difference of $2\nu_{01} = 280 \pm 60\ cm^{-1}$ for the single like C–O bond and $2\nu_{01} = 150 \pm 62\ cm^{-1}$ for the double like C═O bond.

two level model to describe the temperature dependence of the occupation number:[20]

$$\rho(T) = \frac{2}{\exp\left(\frac{2hc\nu_{01}}{kT}\right) + 1} \qquad (2)$$

With this model the temperature dependence of the proton transfer degree determined by neutron single crystal diffraction could be well described.[17] In eqn (2) ν_{01} is the wavenumber of the ground state splitting of the quasi-symmetric potential, which describes the OH stretching motion.

With eqn (1) and (2), fit-functions (3a) and (3b) describing thermal evolution of bond length could be obtained and the energy difference between the two tautomeric forms could be determined.

$$r(\mathrm{C-O}) = \frac{r_{CO} + r_{single}}{2} + \frac{2(r_{CO} - r_{single})}{\exp\left(\frac{2hc\nu_{01}}{kT}\right) + 1} \qquad (3a)$$

$$r(\mathrm{C=O}) = \frac{r_{CO} + r_{double}}{2} + \frac{2(r_{CO} - r_{double})}{\exp\left(\frac{2hc\nu_{01}}{kT}\right) + 1} \qquad (3b)$$

From our data we estimate a ground state splitting of 140 ± 30 cm^{-1} for the thermal evolution of the C–O single bond. From the bond length of the C═O double bond we estimate a ground state splitting of 75 ± 31 cm^{-1}. The quite large difference in the energies determined from the bond lengths in the carboxylic acid is surprising. Nonetheless, a significant difference in the bond lengths of the carboxylic acid group is visible in the room temperature structure of β-9AC. This leads to the hypothesis that proton transfer in β-9AC is more complex than in $KHCO_3$. A plausible ground state splitting of 110 ± 30 cm^{-1} for β-9AC can be estimated.

Computational chemistry of 9AC

The geometry optimization suggests a C_i symmetry for the hydrogen bonded dimer. The calculated harmonic frequencies were scaled by using a scaling factor of 0.9631.[34] The important geometrical parameters of the hydrogen bonded cyclic dimer are shown in Table 2. Apart from the distance of the hydrogen bond $d_{OH\cdots O}$, the theoretical values are in good agreement with the experimental values obtained by X-ray diffraction. The deviation between experiment and theory for the length of the hydrogen bond can be explained by the inadequacy of the X-ray diffraction in determining the position of the protons. Nonetheless packing effects should also be taken into account. These effects can cause an error of 0.1 Å.[35]

Vibrational spectroscopy of β-9AC

The hydrogen bond dynamics lead to a strong temperature dependence of the OH out-of-plane motion, the OH in plane motion, the C═O stretching vibration and OH stretching vibration. With the temperature dependence of these motions the potential of hydrogen bonding can be well described. So we will concentrate on these four motions in the following.

The OH out-of-plane region from 900 to 1000 cm^{-1} exhibits a huge temperature dependence of the intensity, position and line width (see Fig. 7a). During cooling down an additional peak appears at 936.7 cm^{-1} and the bands are blue shifted. The blue shift can be interpreted in terms of a stronger localization of the proton. A comparable behavior was reported for benzoic acid; here the increasing band and the decreasing band were assigned to the OH out-of-plane vibrations of the two tautomers A and B.[36] For the low frequency mode

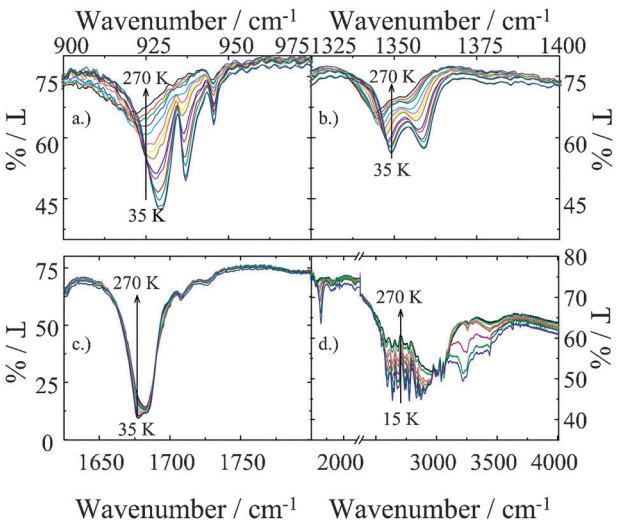

Fig. 7 Temperature dependent FTIR spectra of β-9AC from 270 to 35 K. (a) The in-plane O–H bending region; (b) the out-of-plane O–H bending region; (c) the C═O stretching region; (d) the O–H stretching region.

Table 2 Comparison of theoretical and experimental structural features of the cyclic hydrogen bonded dimer

$d_{O\cdots O}$/Å	$d_{OH\cdots O}$/Å	Bond angle O–C–O	Torsion angle carboxylic group	
2.637	1.63	122.97°	130.4°	Calc. B3PW91/6-311G(d,p)
2.634 ± 0.001	1.72 ± 0.01	(122.7 ± 0.1)°	(125.2 ± 0.2)°	X-ray 75 K

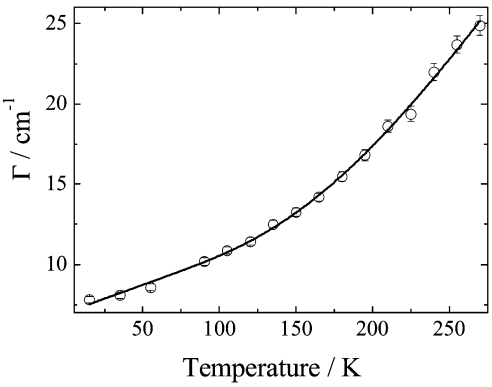

Fig. 8 Temperature dependence of the line width from the O–H out of plane mode. Fit based on eqn (4) results in an activation energy of $E_A = 498 \pm 51$ cm^{-1}.

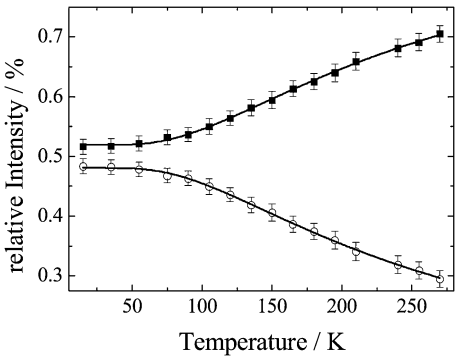

Fig. 9 Temperature dependence of the relative intensities for the OH in plane mode. Fit based on a Fermi–Dirac statistics leading to an energy difference of $2\nu_{01} = 240 \pm 4$ cm^{-1}.

around 920 cm^{-1} the temperature dependence of the line width is shown in Fig. 8. It can be described by a formula given by Carabatos-Nedelec and Becker.[37] The formula is composed of a linear term describing the vibrational relaxation and exponential term characterizing reorientational relaxation of diffuse nature.

$$\Gamma = (a + bT) + C\nu_0 \exp[-E_A/k_B T] \qquad (4)$$

In this formula ν_0 is a "hard-core" wavenumber at critical temperature, a, b and C are empirical parameters modeling the experimental curve and E_A is the activation energy of a reorientational motion. In the case of the OH out-of-plane motion, this activation energy is correlated to the proton transfer in the carboxylic acid dimer. Eqn (4) was recently used for the determination of the activation energies for $-CH_3$, $-NH_2$ and $-NO_2$ reorientation from the line widths in FTIR spectra of 2-methyl-4-nitroaniline.[38] The experimental findings based on vibrational spectroscopy show good agreement with results from NMR spectroscopy and theoretical calculations. The fit based on eqn (4) in Fig. 8 leads to an activation energy of $E_A = 498 \pm 51$ cm^{-1} for the proton transfer in β-9AC. This value fits well to the model-dependent barrier height in benzoic acid,[6,11,12,15] which was determined utilizing QENS and solid state NMR to be in the range of 400–500 cm^{-1}.

The OH in plane motion is shown in the spectral range from 1330 cm^{-1} to 1370 cm^{-1} (see Fig. 7b). The DFT calculation predicts a frequency of 1327.7 cm^{-1} for this mode. The absorption band is composed of two bands, which become sharper at lower temperatures. The relative intensities of both absorption bands show significant temperature dependence (see Fig. 9). This can be described by a Fermi–Dirac statistics, which leads to an energy difference of 240 ± 4 cm^{-1}. According to the electronic structure of the carboxylic acid group our estimated energy difference should be twice the ground splitting of potential for OH stretching motion.[20]

The C=O stretching band is the most intense band in the FTIR spectra at 1681.8 cm^{-1} (see Fig. 7c). DFT calculations predict a frequency of 1684.6 cm^{-1} for this motion. This band also shows temperature dependence in its intensity and could be virtually separated into two bands. The intensity variation for this band is small compared to the OH bending motions.

The OH stretching motion shows a broad and complex absorption band in the FTIR spectra. It covers the spectral region from 2300 cm^{-1} to 3700 cm^{-1} (see Fig. 7d). At 270 K the mean frequency is around 2875 cm^{-1} and shifts during cooling by approximately 50 cm^{-1} to higher frequencies. The DFT calculation predicts a frequency of 3020.0 cm^{-1} for this motion. At lower temperature, a doublet band near the broad OH stretching mode band becomes visible. For benzoic acid, where a similar doublet band is observable,[9] this band was attributed to "zero phonon" transitions. In β-9AC acid we found an intensity ratio of the zero phonon transitions of $I_{1826}/I_{1909} = 2.04 \pm 0.04$. The frequencies of the zero phonon transitions in β-9AC are slightly higher than in benzoic acid. This observation can be explained by a weaker hydrogen bonding in β-9AC compared to benzoic acid. The fine structure of the broad absorption band centered at 2930 cm^{-1} can be explained by coupling with low frequency motions. A complete assignment is beyond the scope of this article. The broadening of this band is related to several mechanisms, like Fermi resonance, Davydov splitting,[39] Evans transmission window[40] and so on. The C–H stretching motions which are also expected in this region can be neglected due to their low oscillator strength. DFT calculations predict these bands at 3068.2 cm^{-1}, 3083.0 cm^{-1} and 3186.9 cm^{-1}. The observed absorption band can be tentatively decomposed into two profiles like in the case of benzoic acid[9] (see Fig. 10). These profiles are centered at 2630 cm^{-1} and 2870 cm^{-1} with an intensity ratio of $I_{2630}/I_{2870} = 2.94$.

The OH stretching can be described by a quasi-symmetric double well potential.[9,10,41,42] This potential function can be written as:

$$V(x) = ax + bx^{2k} + c\exp(-dx^2) \qquad (5)$$

where x is the coordinate of the proton along the O···O bond. The energy levels in this potential have no particular symmetry and they are labeled in the order of their increasing energy. The two absorption profiles can be assigned to the $(2 \leftarrow 0)$ and $(3 \leftarrow 0)$ in this potential. Nonetheless alternative mathematical functions can also be used to describe the proton transfer dynamics.[42] For an accurate determination of the potential a precise measurement of the distance between the two hydrogen sites along the hydrogen bond is necessary. Unfortunately there are no neutron diffraction data available for β-9AC and in the X-ray diffraction the determination of the position of hydrogen atoms is less precise. For a simulation of the ADPs of all hydrogen atoms we used the SHADE web server. Based on the

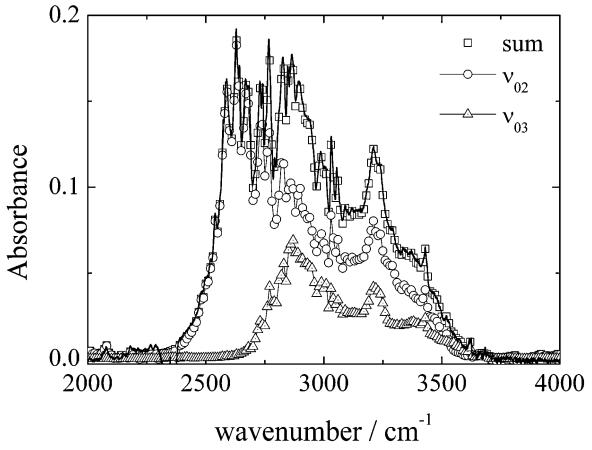

Fig. 10 A tentative decomposition of the absorption profiles of OH stretching motion at 15 K into two comparable absorption bands. Theses bands have an intensity ratio of $I_{2630}/I_{2870} = 2.94$.

combination of these ADPs and our experimental X-ray diffraction data we interpolate a distance of 0.8 ± 0.1 Å between the hydrogen sites at 15 K. This distance is slightly larger than in benzoic acid and $KHCO_3$. Based on this fact, we expect a higher barrier for β-9AC. Finally for the accurate determination of the potential a precise estimation of the ground state splitting ν_{01} is needed. This transition can only be directly determined by applying inelastic neutron scattering (INS).[9] Unfortunately there are no INS data available for β-9AC. Using the thermal evolution of the bond length we could roughly estimate this transition. Using our experimental parameters we estimate a potential function for $k = 1$ shown in Fig. 11. Since the quasi-symmetric potential describes the OH-stretching motion, it should not confused with potential based kinetic investigation shown in Fig. 1. We use the following parameters: $a = 145.25$ Å^{-1} cm^{-1}, $b = 334087$ Å^{-2} cm^{-1}, $c = 271157$ cm^{-1} and $d = 1.529$ Å^{-2}. Table 3 shows experimental and theoretical parameters connected with the potential function. The distance between the two minima has a value of 0.75 Å and is shorter then the experimentally determined distance between two proton sites. This discrepancy can be explained by the nature of X-ray diffraction techniques, which estimates the proton position quite poorly. Since X-ray diffraction monitors the electron density, it can be expected from their electronegativity that bond lengths of polar bonds containing hydrogen atoms are generally too short. Packing effects,[35] which explain the deviation in the bond length between calculated and experimental values, can be excluded, since potential is determined with the experimental spectroscopic properties. The transition ν_{01} obtained from the potential function shows a good agreement with our experimental values estimated from the temperature dependence of the bond lengths in the carboxylic acid group and in the relative intensities of the absorption band assigned as the OH in plane motion. As already explained, the ν_{01} mode can only be observed by INS. It is dominated by the potential asymmetry and can be compared with the tunnel-splitting ν_{0t} for a total symmetric potential. For this case we calculate a splitting of 2.62 cm^{-1}. The INS intensity for the (1 ← 0) transition depends on the delocalization degree ε of the wave function. From our potential we can obtain a delocalization degree $\varepsilon \sim \nu_{0t}/2\nu_{01} \sim 1.27 \times 10^{-2}$. In the case of β-9AC 1.3% of the wave function is delocalized. This value is quite close to the delocalization degree of benzoic acid. This fact leads to the assumption that similar rate constants for the proton transfer in β-9AC can be expected in comparison with benzoic acid. The potential barrier of the quasi-symmetric potential (see Fig. 11) is 5480 cm^{-1}, this value is ten times higher than

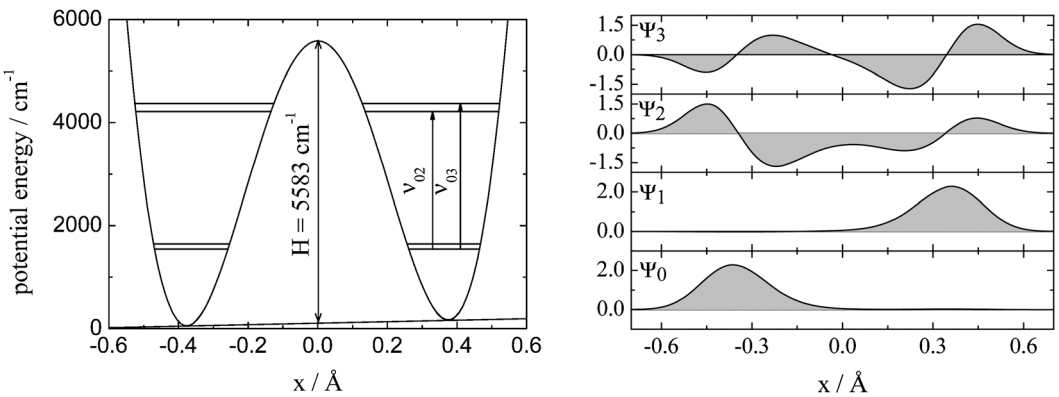

Fig. 11 Estimated potential and wave functions for the OH stretching motion. $V(x) = 145.25x + 334087x^2 + 271157\exp(-1.529x^2)$ (x in Å, V in cm^{-1}).

Table 3 Experimental and theoretical parameters from the estimated potential for OH-stretching motion. $V(x) = 145.25x + 334087x^2 + 271157\exp(-1.529x^2)$

H/cm^{-1}	r/Å	ν_{0t}/cm^{-1}	ν_{01}/cm^{-1}	ν_{02}/cm^{-1}	ν_{03}/cm^{-1}	I_{02}/I_{03}	
5480	0.75	2.62	102.8	2661.2	2820.4	2.94	Theory
n.a.	0.8 ± 0.1	n.a.	(75 ± 31,140 ± 30)[a] 120 ± 2[b]	2630	2870	2.94	Exp.

H is the barrier height, ν_{0t} is the tunnel splitting calculated for the total symmetric potential. [a] From the temperature dependence of the bond length in the carboxylic acid group. [b] From the temperature dependence of OH out of plane motion.

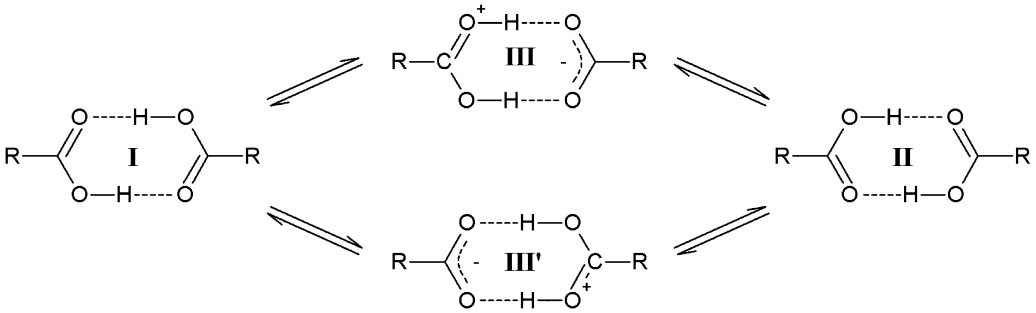

Fig. 12 Schematic illustration of the proton transfer reaction adapted from Fillaux.[6]

activation energy estimated from the line width of the band of the OH out-of-plane motion. Such a high barrier is not surprising since the potential contains the OH-stretching motion with frequencies of 2630 cm^{-1} and 2870 cm^{-1}. One has to consider that the activation energy E_A is connected to the reaction-path model and the quasi-symmetric potential with the high potential barrier is a cornerstone in the coherent tunneling model.[16] The potential barrier of 5480 cm^{-1} is also much higher than the thermal energy. This implies that the proton transfer reaction cannot be understood as an Arrhenius like over-the-barrier process. The wave functions in Fig. 11 show that the lowest states $|0\rangle$ and $|1\rangle$ are strongly localized at one minimum of the quasi-symmetric potential. The lowest minimum represents the initial state **I** of the proton transfer[9] (see Fig. 12). Since the x coordinate of the quasi-symmetric potential represents the proton position along a hypothetical O···O bond, the second minimum corresponds to a superposition of a double protonated dimer **III**, which can be assigned as the intermediate of the proton transfer reaction.[6,9] In this quantum mechanical picture the proton transfer takes place as coherent phonon-assisted tunneling of pseudoprotons.[9,10,20] The temperature dependent transfer rate based on Boltzmann population factors for relevant states is described by three terms.[9]

$$k = 8c\varepsilon\nu_{01}\left[\varepsilon^2 \coth\left(\frac{hc\nu_R}{2k_BT}\right) + \varepsilon\exp\left(-\frac{hc(\nu_{01}-\nu_R)}{k_BT}\right) + \exp\left(-\frac{hc(2\nu_{01}+\nu_R)}{k_BT}\right)\right] \quad (6)$$

First the sum of the up and down phonon rates is represented by the $\coth(h\nu_R/2k_BT)$ term. The frequency ν_R is a quasi-harmonic lattice mode, which is correlated to the proton transfer.[9,20] For benzoic acid this frequency was determined to be (54 ± 6) cm^{-1}[19] and for 9AC a similar frequency for this mode can be assumed. The second term and the third term are Arrhenius like expressions. The activation energy in these terms is related to the ground state splitting of the quasi-symmetric potentialν_{01} and the quasi-harmonic lattice mode ν_R. This leads to the following terms $\exp(-hc(\nu_{01}-\nu_R)/k_BT)$ and $\exp(-hc(3\nu_{01}+\nu_R)/k_B\ T)$.[9,20] The sum $2\nu_{01}+\nu_R$ would give a value quite close to activation energy based on line widths of OH out-of-plane motion. With parameters of benzoic acid[9] the rate constant is dominated by the third term at roughly 100 K leading to an Arrhenius like behavior. Nonetheless it is also necessary to be aware that the temperature dependence of the line widths is not fitted with a simple Arrhenius approach. The fit function consists of a classical Arrhenius approach and a linear term describing the vibrational relaxation. It is easy to understand that the vibrational relaxation dominates at low temperature. One has to take into account that the term for vibrational relaxation influences the determined activation energy. Furthermore the line widths also depend on resolution of the spectrometer. The potential barrier and the activation energy both are physically relevant quantities in this hydrogen bonded system. In the coherent tunneling model the proton transfer can be described for high temperatures in terms of a classical Arrhenius behavior with an activation energy E_A = 498 ± 51 cm^{-1}.

Conclusion

The hydrogen bonding in β-9AC causes a dynamical disorder, which is visible in the high resolution X-ray diffraction data. From the temperature dependence of the bond lengths in the carboxylic acid group we could extract thermodynamic properties describing the proton transfer in the carboxylic acid dimer. The crystallographic findings were compared with results from FTIR spectroscopy. The vibrational spectroscopy shows comparable results to other dimeric carboxylic acids in the solid state like benzoic acid. Our experimental findings add another piece to the understanding of hydrogen bond dynamics in carboxylic acid dimers. Our main conclusions are summarized in the following:

1. The crystallographic results with an intermolecular distance of 2.636 Å between the oxygen atoms at 50 K suggest a weaker hydrogen bond in β-9AC compared with benzoic acid.

2. From the temperature dependence of the length of the carbon–oxygen bonds the energy differences of the potential tautomers could be determined to be $2\nu_{01}$ = 220 ± 70 cm^{-1}.

3. From the line width of the OH out-of-plane motion it was possible to extract an activation energy of 498 ± 51 cm^{-1}. This activation energy based on a classical Arrhenius approach is comparable to the activation energy for other carboxylic dimers in the solid state found by quasi elastic neutron scattering and solid state NMR.

4. From the relative intensities of the absorption bands of the OH in plane motion we estimate an energy difference of $2\nu_{01}$ = 240 ± 4 cm^{-1} utilizing Fermi–Dirac statistics. This value is comparable with our crystallographic results.

5. Our estimated potential for OH-stretching motion has a barrier height of 5480 cm^{-1}. This value is ten times larger than

the activation energy obtained from the line width. In the quantum mechanical picture the proton transfer takes place as a phonon assisted coherent tunneling between the states $|0\rangle$ and $|1\rangle$ in quasi-symmetric potential. This implies that the tunneling matrix element ν_{0t}, the ground state splitting ν_{01} and the delocalization degree of the wave function $\varepsilon \sim \nu_{0t}/\nu_{01}$ are the key parameters for the proton transfer reaction.[9]

Acknowledgements

This work has been supported by the Deutsche Forschungsgemeinschaft (DFG) *via* SFB 602. We thank DESY (Beamlines F1 and D3) and the ESRF (Beamlines ID09b and ID11) for experimental support. The authors thank Jürgen Bienert for his assistance with the FTIR and Reza Kia for the helpful discussions.

References

1 W. M. Latimer and W. H. Rodebush, *J. Am. Chem. Soc.*, 1920, **42**, 1419.
2 S. N. Vinogradov and R. H. Linnell, *Hydrogen Bonding*, Van Nostrand Reinhold Company, New York, 1971.
3 P. Schuster, *Hydrogen Bonds*, Springer Verlag, Berlin, 1984, vol. 120.
4 A. S. F. Ramos and S. Techert, *Biophys. J.*, 2005, **89**, 1990.
5 C. Emmeluth and M. A. Suhm, *Phys. Chem. Chem. Phys.*, 2003, **5**, 3094.
6 F. Fillaux, *Int. Rev. Phys. Chem.*, 2000, **19**, 553.
7 J. P. Ceron-Carrasco, J. Zuniga, A. Requena, E. A. Perpete, C. Michaux and D. Jacquemin, *Phys. Chem. Chem. Phys.*, 2011, **13**, 14584.
8 F. Duarte, E. Vohringer-Martinez and A. Toro-Labbe, *Phys. Chem. Chem. Phys.*, 2011, **13**, 7773.
9 F. Fillaux, M. H. Limage and F. Romain, *Chem. Phys.*, 2002, **276**, 181.
10 F. Fillaux, F. Romain, M. H. Limage and N. Leygue, *Phys. Chem. Chem. Phys.*, 2006, **8**, 4327.
11 J. L. Skinner and H. P. Trommsdorff, *J. Chem. Phys.*, 1988, **89**, 897.
12 B. H. Meier, F. Graf and R. R. Ernst, *J. Chem. Phys.*, 1982, **76**, 767.
13 J. Seliger, V. Zagar, K. Gotoh, H. Ishida, A. Konnai, D. Amino and T. Asaji, *Phys. Chem. Chem. Phys.*, 2009, **11**, 2281.
14 J. M. Clemens, R. M. Hochstrasser and H. P. Trommsdorff, *J. Chem. Phys.*, 1984, **80**, 1744.
15 A. J. Horsewill and A. Aibout, *J. Phys.: Condens. Matter*, 1989, **1**, 9609.
16 F. Fillaux, A. Cousson and M. J. Gutmann, *Pure Appl. Chem.*, 2007, **79**, 1023.
17 F. Fillaux, A. Cousson and M. J. Gutmann, *J. Phys.: Condens. Matter*, 2006, **18**, 3229.
18 C. C. Wilson, N. Shankland and A. J. Florence, *J. Chem. Soc., Faraday Trans.*, 1996, **92**, 5051.
19 C. C. Wilson, N. Shankland and A. J. Florence, *Chem. Phys. Lett.*, 1996, **253**, 103.
20 F. Fillaux, *J. Mol. Struct.*, 2007, **844–845**, 308.
21 Y. Ito and H. Fujita, *J. Org. Chem.*, 1996, **61**, 5677.
22 R. O. Al-Kaysi and C. J. Bardeen, *Adv. Mater.*, 2007, **19**, 1276.
23 L. Y. Zhu, R. O. Al-Kaysi and C. J. Bardeen, *J. Am. Chem. Soc.*, 2011, **133**, 12569.
24 L. Y. Zhu, R. O. Al-Kaysi, R. J. Dillon, F. S. Tham and C. J. Bardeen, *Cryst. Growth Des.*, 2011, **11**, 4975.
25 R. Moré, G. Busse, J. Hallmann, C. Paulmann, M. Scholz and S. Techert, *J. Phys. Chem. C*, 2010, **114**, 4142.
26 J. Hallmann, W. Morgenroth, C. Paulmann, J. Davaasambuu, Q. Y. Kong, M. Wulff and S. Techert, *J. Am. Chem. Soc.*, 2009, **131**, 15018.
27 W. Kabsch, *Acta Crystallogr., Sect. D: Biol. Crystallogr.*, 2010, **66**, 125.
28 G. M. Sheldrick, *Acta Crystallogr., Sect. A: Found. Crystallogr.*, 2008, **64**, 112.
29 M. J. Frisch, G. W. TrucksH. B. Schlegel, G. E. Scuseria, M. A. Robb, J. R. Cheeseman, G. Scalmani, V. Barone, B. Mennucci, G. A. Petersson, H. Nakatsuji, M. Caricato, X. Li, H. P. Hratchian, A. F. Izmaylov, J. Bloino, G. Zheng, J. L. Sonnenberg, M. Hada, M. Ehara, K. Toyota, R. Fukuda, J. Hasegawa, M. Ishida, T. Nakajima, Y. Honda, O. Kitao, H. Nakai, T. Vreven, J. A. Montgomery, Jr., J. E. Peralta, F. Ogliaro, M. Bearpark, J. J. Heyd, E. Brothers, K. N. Kudin, V. N. Staroverov, R. Kobayashi, J. Normand, K. Raghavachari, A. Rendell, J. C. Burant, S. S. Iyengar, J. Tomasi, M. Cossi, N. Rega, J. M. Millam, M. Klene, J. E. Knox, J. B. Cross, V. Bakken, C. Adamo, J. Jaramillo, R. Gomperts, R. E. Stratmann, O. Yazyev, A. J. Austin, R. Cammi, C. Pomelli, J. W. Ochterski, R. L. Martin, K. Morokuma, V. G. Zakrzewski, G. A. Voth, P. Salvador, J. J. Dannenberg, S. Dapprich, A. D. Daniels, Ö. Farkas, J. B. Foresman, J. V. Ortiz, J. Cioslowski and D. J. Fox, *Gaussian09*, Gaussian, Inc., Wallingford, CT, 2009.
30 A. O. Madsen and S. Larsen, *Angew. Chem., Int. Ed.*, 2007, **46**, 8609.
31 S. Tsuzuki and H. P. Luthi, *J. Chem. Phys.*, 2001, **114**, 3949.
32 A. O. Madsen, *J. Appl. Crystallogr.*, 2006, **39**, 757.
33 P. Munshi, A. O. Madsen, M. A. Spackman, S. Larsen and R. Destro, *Acta Crystallogr., Sect. A: Found. Crystallogr.*, 2008, **64**, 465.
34 M. Govindarajan, K. Ganasan, S. Periandy and S. Mohan, *Spectrochim. Acta, Part A*, 2010, **76**, 12.
35 J. Moellmann and S. Grimme, *Phys. Chem. Chem. Phys.*, 2010, **12**, 8500.
36 S. Hayashi and J. Umemura, *J. Chem. Phys.*, 1974, **60**, 2630.
37 C. CarabatosNedelec and P. Becker, *J. Raman Spectrosc.*, 1997, **28**, 663.
38 U. Okwieka, K. Holderna-Natkaniec, T. Misiaszek, W. Medycki, J. Baran and M. M. Szostak, *J. Chem. Phys.*, 2009, **131**.
39 I. D. Mikhailov, V. A. Savelev, N. D. Sokolov and N. G. Bokii, *Phys. Status Solidi B*, 1973, **57**, 719.
40 J. C. Evans, *Spectrochim. Acta*, 1962, **18**, 507.
41 F. Fillaux, *Chem. Phys.*, 1983, **74**, 405.
42 R. L. Somorjai and D. F. Hornig, *J. Chem. Phys.*, 1962, **36**, 1980.